

# Frequency-Band Analysis of Equalization Enhanced Phase Noise Jointly with DSP Impact

C. S. Martins,<sup>1</sup> A. Lorences-Riesgo,<sup>1</sup> S. Mumtaz,<sup>1</sup> T. H. Nguyen,<sup>1</sup> A. Hraghi,<sup>1</sup>  
Z. Wu,<sup>1</sup> Y. Frignac,<sup>1</sup> G. Charlet,<sup>1</sup> and Y. Zhao<sup>1</sup>

<sup>1</sup> Huawei Technologies France, Paris Research Center, Optical Communication Technology Lab,  
Boulogne-Billancourt, France

\* celestino.sanches.martins@huawei.com

**Abstract:** The fundamental of equalization-enhanced phase noise (EPPN) jointly with the DSP impact is investigated, using an approach based on frequency-band segmentation of the frequency-noise (FN) spectrum. This approach enables to study the EPPN penalty of different FN spectral regions and correlated with its bursty nature. © 2023 The Author(s)

## 1. Introduction

In advanced coherent optical transmission systems, the interplay between the phase noise of local oscillator (LO) laser and digital chromatic dispersion (CD) compensation (CDC) can result in a significant system penalty named as equalization enhanced phase noise (EPPN) [1]. Research on this topic has been extensively conducted [1–6], revealing that this penalty arises as timing jitter from the frequency noise conversion as well as an additional noise process. In [2], it was analyzed multiple regimes division of a general non-white frequency noise spectrum, referring that each regime may impose different set of impairment, thus providing different design criteria. Recently, it was discussed the system impact of EPPN for different baud-rate and transmission distance in single-carrier system along with the bursty nature of frequency noise [3].

In this paper, we further extend the study on the EPPN penalty on single-carrier signals, by partitioning the frequency noise spectrum into different frequency bands and quantifying the EPPN penalty on each band separately. In addition, we evaluate the impact of DSP modules including multi-input-multi-output (MIMO) Equalizer and timing recovery (TR) on per frequency-band EPPN penalty. We show that the tracking bandwidth design of MIMO and TR is important for the burst error characteristics.

## 2. Experimental Analysis of EPPN Penalty

In this section we experimentally investigate the EPPN penalty and its corresponding burst error using a 95 Gbaud single-carrier transmission system using the experimental setup shown in Fig. 1. We generate a dual-polarization PCS-64QAM signal with 5 bit/symbol entropy and combine it with another 20 WDM channels emulated by ASE noise and spaced by 100 GHz. The transmission link consists of 15 heterogeneous spans, with a total distance of 1340 km and 26 ns/nm of accumulated dispersion. After the link, we filter the channel under test before the coherent receiver. Offline DSP includes front-end compensation, dispersion compensation, equalization and carrier recovery. After DSP, the signal SNR is evaluated as performance metric.

Fig. 2 shows the evolution of SNR over time for an illustrative understanding of EPPN penalty effect and its possible corresponding burst error. The SNR estimation is performed over 500M symbols, divided into segments, in which we name as estimation block-size. Note that this estimation block-size refers to the interleaving length of FEC as in described [3]. Besides, two types of commercial lasers, distributed Bragg reflector (DBR) and External Cavity Laser (ECL), have been used both in transmitter and receiver side. In this regard, the performance for

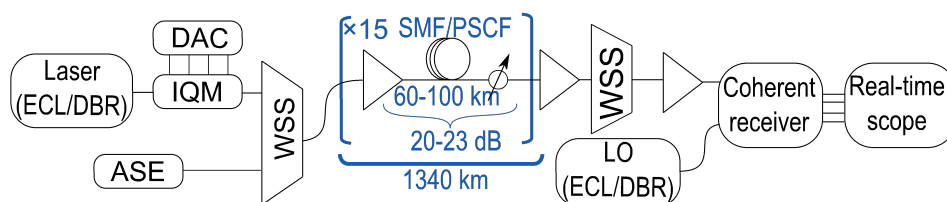


Fig. 1: Experimental setup of the 21×95 GBaud WDM PCS-16QAM single-carrier transmission system.

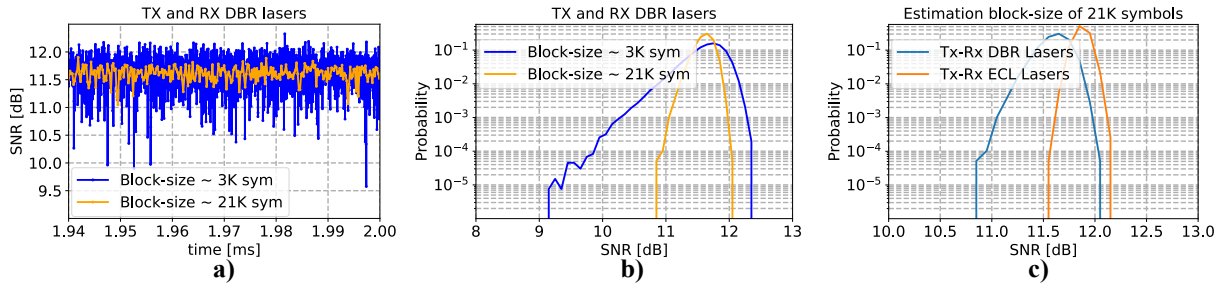


Fig. 2: a) SNR evolution over time for block-size estimation of 3K and 21K symbols using DBR lasers at both Tx and Rx; b) and c) PMF characterization for the SNR distribution: b) for different block-size estimation; c) comparing DBR-DBR and ECL-ECL transmitter- and receiver-side lasers combination.

different estimation block-size is presented in Fig. 2 a), considering 3K and 21K symbols and using DBR lasers at both Tx and Rx. We can observe frequent drop of SNR over time which can be the cause of burst error, studied in [3]. Also note that increasing block-size provides less drop, being in accordance with [3]. In addition, we have also performed the characterization of burst error based on the probability mass function (PMF) in Fig. 2 b) and c), considering different estimation block-size and lasers type, respectively. The probability is calculated over 0.1 dB of SNR range. In Fig. 2 b), we can note the probability of larger burst error events for 3K block-size, while for 21K symbols estimation block-size the SNR spread is significantly reduced. From Fig. 2 c), we can observe that using ECL lasers do now show a burst behavior since the SNR varies in an about 0.5 dB range.

### 3. Simulation Study for the Fundamental of EEPN Penalty

In this section, we proceed with a fundamental analysis on the EEPN penalty and burst errors described in the previous section based on simulation. The frequency noise of DBR laser in the lab is measured and loaded in the laser model of simulation platform. The simulation setup aims for analysis of upcoming generation transceiver operating at 195 Gbaud. In order to attain a comprehensive insight on the EEPN penalty and burst errors, we propose to divide the FN power spectrum density (PSD) into several spectral bands, then followed with the per-band EEPN penalty evaluation. This, in turn, enables us to understand the frequency-dependent behavior of EEPN noise, which can give us a clear hint about how to jointly design the laser and optimize the DSP modules, so that the EEPN penalty and burst error risk are reduced. Note that this approach is aligned with the analysis provided in [2] regarding different regimes of laser FN spectrum causing different impairments, however in this work we further provide per frequency-band EEPN penalty evaluation.

Within this framework, Fig. 3 a) presents the frequency-band dependent evolution of EEPN penalty, for the FN spectrum split in 16 bands and considering the following DSP modules: MIMO equalizer for various updating speed via tuning the convergence coefficient  $\mu$  and TR using different tracking bandwidth set by its delay. The TR algorithm considered in this study is based on the traditional Gordard algorithm [7]. It is worth mentioning that the influence on the number of bands for FN spectrum is negligible on the main results conclusions. For the sake of analysis simplicity, in Fig. 3 a) we have considered three segmented areas for an overall EEPN penalty, corresponding to low, middle and high frequency regions of FN PSD, similarly to the previous study performed in [2]. The segmentation is determined mainly by the CD bandwidth, i.e., the inverse of channel memory due to CD. Note that for 195Gbaud signal and CD of 60 ns/nm, CD bandwidth is around  $\approx 10.7$  MHz. The low frequency region is the zone where the frequency is static compared to the CD bandwidth, and the EEPN noise is mainly caused by the conversion of optical frequency variation of LO laser to the timing error through the digital CDC. This impairment can be partially handled by proper design of MIMO equalizer but generally more effectively by TR, due to the high tracking bandwidth of TR. For instance, as shown in Fig. 3 a), by turning the TR off, and increasing 10 times the updating speed of MIMO equalizer via tuning the convergence coefficient  $\mu$ , enables to significantly reduce the penalty, given its increasing tracking bandwidth to around 10 times. Similarly, we have also evaluated two configuration of TR: TR-1 and TR-2, where the tracking bandwidth of TR-1 is 10 times higher than TR-2. Therefore, we can also notice that TR-1 can achieve much better EEPN penalty tolerance. Calculation of equalizer an TR tracking bandwidth may not be straightforward since it depends on loop latency and others ASIC specificity, nevertheless at 195 Gbaud, we can roughly estimate for MIMO  $\mu = 10^{-5}$  and  $\mu = 10^{-4}$ , as  $\approx 2$  MHz and  $\approx 20$  MHz, respectively.

On the other hand, the middle region, corresponding to the frequency range near to CD bandwidth, reveals to be the zone of interest where the peak of the EEPN penalty tends to occurs. In this region the EEPN penalty due to the interaction between digital CDC and the phase noise is not only a timing jitter problem, and therefore more

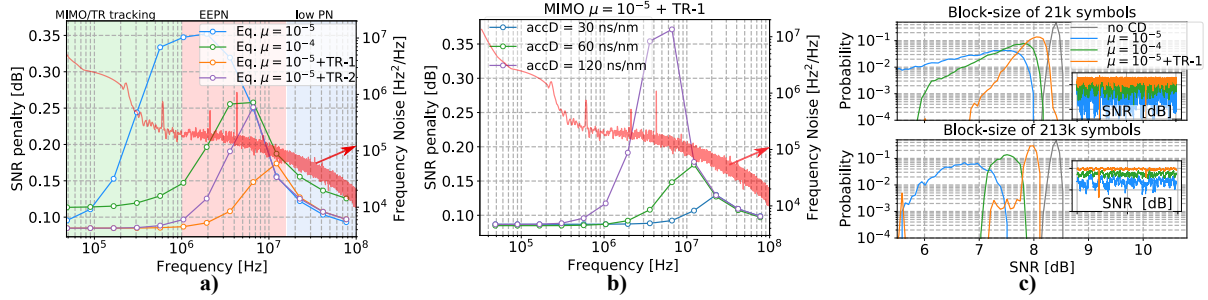


Fig. 3: a) and b) EEPN penalty evolution as a function of frequency divided in 16 bands of laser FN spectrum considering: a) accumulated dispersion (accD) of 60 ns/nm; b) accumulated dispersion of 30 ns/nm, 60 ns/nm and 120 ns/nm; c) PMF characterizing the estimated SNR distribution for different DSP modules using accD of 60 ns/nm.

challenging to be compensated for. To emphasize this, We have also evaluated three different dispersion values shown in Fig. 3 b), where  $\mu = 10^{-5}$  and TR is turned on, the penalty tends to increase as the band frequency advance toward CD bandwidth, i.e.,  $\approx 10.7$  MHz at 60 ns/nm. Also note that the peak of EEPN penalty is shifting according to their respective CD bandwidth. On its turn, in the high frequency region, the phase noise evolution tends to be increasingly lower, therefore, imposing a reducing penalty.

In Fig. 3 c) we present the PMF characterization for the estimated SNR distribution considering equalizer with different MIMO updating speed and TR-1 configuration, using two different estimation block-size of 21K and 213K symbols, over 20M symbols. Also, baseline distribution curve with no CD is also included. In this analysis we aim to link the impact of DSP modules and estimation block-size on SNR distribution in Fig. 3 c) with the frequency-band dependent evolution of EEPN penalty in Fig. 3 a). Primarily, we see that DSP modules with higher tracking bandwidth enables lower SNR variation, which in turn reduces the large drops in time span observation and consequently the probability of larger burst error events. On the other hand, we note that the probability of larger burst error increases with decreasing estimation block-size due to its larger SNR variation in PMF. This can be intuitively explained by interpreting a low-pass filtering bandwidth for the estimation block-size being inversely proportional to its size. In this sense, the block-size of 21K and 213K symbols correspond to  $\approx 10$  MHz and  $\approx 1$  MHz, respectively. This means that increasing estimation block-size imposes a reduction on the accumulated penalty on frequency-band dependent evolution of EEPN penalty curve, since the penalty is integrated for frequencies up to around the frequency given by the inverse of the block size duration.

#### 4. Conclusion

We have evaluated the EEPN penalty over segmented FN spectrum into several bands together with the impact of MIMO and TR bandwidth. We show that the most important frequency region of FN is dependent of CD. We also analyze the correlation between EEPN penalty and the bursty nature phenomena of FN for different system design aspect, including FEC interleaving length impact. Overall, the frequency-band dependent EEPN penalty evaluation can be relevant for jointly optimize the laser design and DSP modules implementation.

#### References

1. W. Shieh, K. P. Ho, "Equalization-enhanced phase noise for coherent-detection systems using electronic digital signal processing," in *Opt. Express*, 16, 15718–15727, (2008).
2. Kakkar, A., Rodrigo Navarro, J., et al., "Resonant THz-meshes," *Nature Sci Rep* 7, 844 (2017).
3. H. Xu, M. O. Rebellato and S. -C. Wang, "System Impact of Laser Phase Noise On 400G And Beyond Coherent Pluggables," in *OFC*, 2012, OTh4C.1.
4. H. Sun and K. Wu, "Clock Recovery and Jitter Sources in Coherent Transmission Systems," in *OFC*, 2023, Th1E.1.3.
5. S. Oda et al, "Interplay between local oscillator phase noise and electrical chromatic dispersion compensation in digital coherent transmission system," in *ECOC*, 2010.
6. R. Zhang, W. et al, "Laser Frequency Jitter Tolerance and Linewidth Requirement for  $\geq 64$ Gbaud DP-16QAM Coherent Systems," in *OFC*, 2019.
7. D. Godard, "Passband timing recovery in an all-digital modem receiver," in *IEEE Trans. Commun.*, 26(5), 517–523 (1978).